A hybrid optimisation approach to improve long-term performance of enhanced geothermal system (EGS) reservoirs

Samin, Maleaha; Faramarzi, Asaad; Jefferson, Ian; Harireche, Ouahid

DOI:
10.1016/j.renene.2018.11.045

A Hybrid Optimisation Approach to Improve Long-Term Performance of Enhanced Geothermal System (EGS) Reservoirs

Samin, Maleaha; Faramarzi, Asaad; Jefferson, Ian; Harireche, Ouahid

DOI:
https://doi.org/10.1016/j.renene.2018.11.045

A Hybrid Optimisation Approach to Improve Long-Term Performance of Enhanced Geothermal System (EGS) Reservoirs

Maleaha Y. Samin[1], Asaad Faramarzi[1], Ian Jefferson[1], Ouahid Harireche[2]

[1] Civil Engineering Department, School of Engineering, University of Birmingham, UK

[2] Civil Engineering, Islamic University of Medina, Medina, Kingdom of Saudi Arabia

Abstract

Improving the long-term performance of deep geothermal reservoirs, as an energy source, can lead to a significant increase in efficiency of heat extractions from these assets. This will assist designers, energy firms, managers, and government decision makers to plan and maintain the use of limited available energy resources and hence enhance key sustainable development goals. Enhanced geothermal reservoirs possess a multi-phase behaviour with complex inter-relationship between several parameters that makes the analysis and design of these systems challenging. Often, this challenge is increased when taking into consideration the optimum use of the available resources and induced costs during both creation and exploitation phases. This research presents a novel design approach developed to achieve efficiency and improved long-term performance in doublet enhanced geothermal systems (EGS). The proposed approach is based on an optimisation procedure using a numerical hybrid methodology integrating a multi-objective genetic algorithm with finite element analysis of fully coupled thermal hydraulic processes of reservoirs. The results of the optimisation process are discussed in comparison with data available from a benchmark case study. The results demonstrate a significant improvement in the long-term performance of EGS reservoir, both in terms of thermal power and costs when optimised using the proposed methodology.

Key words: Enhanced geothermal system; optimisation; finite element method; thermal drawdown; thermal power production

1 Introduction

Geothermal power has been used for many centuries but, mostly extracted from shallow sources and natural hot springs [1]. It is, however, only recently that the technology to exploit hot-dry-rock (HDR) geothermal reservoirs has advanced sufficiently. In 1974, the first HDR deep geothermal reservoir in Los Alamos was developed, where the heat of the subsurface at the depth of between 4 to 5 kilometres was extracted to generate electricity power [2]. This was followed by trials of HDR in the UK at the Rosemanowes Quarry between 1977-1980 [3]. However, the modern process of extracting heat from a deep geothermal reservoir stems from developments in the 1990s where a hot dry rock matrix was stimulated using hydraulic fracturing at depths over 2.5 kilometres where temperatures of 150-200 °C exist. This resulted into the development of the so called Enhanced Geothermal System (EGS) [4], where energy in the form of hot fluid or steam can be produced.

In general, geothermal energy, due to its nature, is much more predictable than other renewable sources of energy; hence it is a popular option in many countries [5]. For example, in China it is predicted that geothermal reservoirs have the potential to produce enough energy for over 5000 years of China's annual total energy consumption (i.e. 95.2×1018Joules in 2010), if just 2% of its EGS resources are recovered [6]. However, due to requirements in advanced technology and economic challenges, as well as uncertainties that exist at the depths used for EGS [7, 8], EGS is still considered to be at the 'proof of concept' stage [9]. These challenges have resulted in deserting many geothermal projects, e.g. the Spa Urach project, Germany, which started in 1977 but was abandoned in 1981 due to financial problems [10]. Other examples include the Basel Project in Switzerland and Southeast Geysers in the USA, where they were abandoned because of technical difficulties, see [11] and [12]. Another key challenge that faces EGS reservoirs is the time taken by the cold fluid front to reach the production well, known as the thermal breakthrough [13]. This problem was first identified by Gringarten and Sauty [13] during development of an analytical model for a sedimentary reservoir to optimise the distance between the injection and production wells in a doublet system with a constant heat for long term production. The thermal breakthrough of the reservoir has been observed in existing projects such as the geothermal reservoir in the UK at Rosemanowes Quarry [14] and the Hijiori hot dry reservoir in Japan [15], which led to abandoning both projects.

Due to significant costs involved in field trials of HDR reservoirs [7], computational modelling is deemed to be an affordable option to enable researchers to investigate possible ways to extend the use of EGS particularly during the preliminary stages to assess the thermal power and the economic feasibility of EGS sites [7]. A comprehensive study conducted by [16] on numerical modelling of EGS reservoirs, indicated that, in general, modelling can be divided into three different categories in terms of EGS reservoir performance. The first category relates to improving the efficiency of heat extraction technologies for different rock deposits considering a wide range of contributing temperatures. The second category aims to evaluate the commercial feasibility of the extracted thermal energy at various stages of designing prospective resources. The third category estimates the thermal performance of existing and potential future EGS reservoirs based on the initial thermal energy extraction rate [16]. In recent decades, different researchers have proposed a variety of numerical modelling strategies to gain an understanding and explore potential trade-off of the above three key categories [17-20]. These studies offered some understanding, interpretation and insights into the complex processes taking place in specific EGS reservoirs. However, they did not probe directly the reservoir design parameters that influence the long-term performance of EGS reservoirs [16].

Recently, several studies have used optimisation approaches in order to achieve efficiency in one or more aspects of EGS performance. Chen and Jiang [21], used a parametric study to analyse the optimum design of an EGS multi-wells reservoir. They found that the configuration of production wells in relation to the injection well affects the reservoir efficiency in terms of heat extraction. However, they did not consider the change in the distance between the injection and production wells, whilst it has been shown that this parameter has a significant impact on the reservoir efficiency as stated by [13, 22, 23]. Biagi et al. [24], used a multi-objective genetic algorithm to optimise injection flow rate of Carbone dioxide (CO_2) as a working fluid in a geothermal reservoir. The optimisation technique was used to reduce the impact of CO_2 on the environment in addition to the increase of the power generation for the long-term performance of EGS reservoirs. Their work can be considered as a management model assessment tool of the existing sites rather than a way to design EGS reservoirs during the early decision stages. Chen et al. [23], used a Multivariate Adaptive Regression Spline (MARS) based statistical model to optimise well positions of a potential geothermal reservoir near Superstition Mountain in Southern California, USA. They found that the MARS model provides significant improvement when dealing with the uncertainty of design parameters. Li et al. [25], optimised the design of an EGS based on the calculation of heat extraction efficiency for long-term performance using finite element analysis and parametric study of a doublet horizontal wells reservoir. However, they have not considered the impact of costs over the life of reservoir. Aliyu and Chen [26], conducted a sensitivity analysis on the impact of artificial and natural design parameters of Soultz reservoir on its long-term performance. They concluded that the long-term performance of EGS can be enhanced through a strong control of the investigated parameters, such as temperature and pressure of the injected fluid. However, to make a decision during the preliminary stage to design a reservoir, there is still a need to develop a new systematic approach that combines all design parameters in one model. In addition, in previous studies, inter-relationships of contributing parameters are usually ignored; such oversimplification has been shown to be insufficient to explain the overall reservoir behaviour [26]. The impact and interaction between reservoir parameters that influence the overall performance, including the total power and breakthrough time, are far more complex than simply considering these in isolation.

Therefore, it is clear that commercial EGS should combine both design and post-design models in order to achieve an efficient system. Thus, this has motivated the proposal of the novel approach presented in this paper to optimise both design and management of EGS reservoirs using a hybrid optimisation technique. This study integrates finite element (FE) analysis and genetic algorithm (GA) optimisation technique, to evaluate the influence of design parameters in order to achieve optimal EGS reservoir design. Via this approach, it will be possible to choose an optimum EGS reservoir design, considering various key parameters as input variables, with respect to the heat extraction efficiency, commercial feasibility and reservoir long-term performance. Whilst there are several factors that have impact on the long-term heat production of an EGS reservoir, it is vital to identify key contributing parameters to ensure suitability of the proposed project. It should be noted that the present study will focus on applying the proposed technique to the heat extraction process of reservoirs. Results may vary should other aspects of the system (e.g. energy conversion system on ground) be included in the analyses as reported by Zhang et al., 2013 [27].

2 Methodology and model development

2.1 Integration of the Finite element method with genetic algorithm optimisation

The methodology used in the research presented in this paper is based on a combination of a coupled heat and mass transfer finite element (FE) procedure with a multi objective genetic algorithm (GA), to optimise efficiency and performance of enhanced geothermal reservoirs. In this approach, firstly, finite element models of EGS reservoir are built using randomly selected representative parameters via a multi-objectives optimisation algorithm. Several scenarios are generated to model an EGS system using the FE method and each model is evaluated against a set of criteria (i.e. optimisation objectives). Successful models are taken forward while those models diverging from the optimisation objectives are abandoned in the next generations. New models are generated using combinations of bioinspired natural selection functions available in the GA. This process continues until an acceptable tolerance or maximum number of generations (both defined by the user) have been achieved. The proposed hybrid approach (i.e. combined FE and GA) allows the exploration of a wide range of FE models to investigate long-term performance of reservoirs in an efficient and intelligent manner – performing such analysis using an ordinary FE method alone is unfeasible [28]. Figure 1, shows a flowchart that describes the process. Further details about the proposed hybrid optimisation approach, and genetic algorithm in general, can be found in Faramarzi et al. [29].

Figure 1. Flowchart for the integration of FE Analysis with Multi-objective GA

Based on the previous studies and taking into account the long-term performance of EGS reservoirs, three optimisation objectives are considered in this study; (i) thermal drawdown, (ii) accumulative thermal power, and (iii) total reservoir cost. These objectives have been selected for optimisation in this research based on the literature (e.g. [30-32]). Each of these optimisation objectives are briefly described below:

i. Thermal drawdown (*TD*): this parameter is defined as the declination ratio of the production temperature during heat extraction and it is used to predict the reservoir thermal breakthrough time [13]. *TD* is calculated using Eq. 1[13]:

$$TD = \frac{T_p - T_\circ}{T_{inj} - T_\circ} \tag{1}$$

Where, T_p, T_o and T_{inj} (°C) are the production, initial and injected fluid temperature (°C), respectively. To avoid encountering thermal breakthrough in a reservoir, it has been suggested that thermal drawdown must not reach 10% [13, 33, 34]. To account for this important performance criterion [30], 10% of *TD* is considered as the threshold value during the optimisation process used in this study.

ii. The thermal power (W_{hp}) is defined as the heat production power of the EGS and is calculated based on the first law of Thermodynamics [31], see Eq. 2:

$$W_{hp} = q(h_p - h_{inj}) \tag{2}$$

Where h_p and h_{inj} (J/kg) are the production and injection specific enthalpies and q (kg/s) is the mass flow rate of the fluid. The accumulative thermal power is calculated up to the end of the reservoir service life, which occurs at the breakthrough time, where the thermal power (W_{hp}) of the reservoir is assumed to be zero at 10% of *TD* [33]. The accumulative thermal power is ($\sum W_{hp}$) calculated using Eq. 3:

$$\sum W_{hp} = \sum_{t=0}^{J} W_{hp} \tag{3}$$

J (years) is the number of years at the reservoir breakthrough time; t (years) is the time of operation.

iii. The third optimisation objective is the total cost of EGS. The high capital cost of geothermal reservoirs and particularly the drilling cost of EGS reservoirs is the main challenge that prevents the geothermal power to move from the 'proof of concept' stage [9] to become a commercially feasible source of energy. The total cost of a reservoir is defined into two parts: the creation cost and the operation cost over time. This is explained in details below:

Creation cost: drilling cost has the highest fraction of the total capital cost of the creation stage [32]. According to Tester and Herzog [35], the drilling cost is ranged anything from 42% to 95% of the power plant total creation cost of EGS reservoirs and it is a function of the reservoir depth. Lukawaski *et al.* [36], suggested that the drilling cost of each well in the reservoir can be calculated using Eq. 4 [36]:

$$Geothermal\ well\ cost\ (C_w) = 1.72 * 10^{-7} * {D_h}^2 + 2.3 * 10^{-3} * D_h - 0.62 \tag{4}$$

Where, D_h (m) is the depth of the reservoir base. Eq. 4 shows that the drilling cost increases non-linearly with the increase in the reservoir depth.

Operation Cost: The operation cost of heat extraction (C_e) of an EGS reservoir is calculated based on the following Equation by Kong *et al.* [37].

$$Ce = Q.\sum_{t=0}^{J}\frac{(\Delta P.pp + \rho_l.c_l.\Delta T.pr.\eta)_t}{(1+r)^t} \quad (5)$$

Where Q (m^3/s) is the exploited fluid volume; ΔP (Pa) is the pressure change at the production well, *pp* (US$/kWh) is the electrical power price, *pr* (US$/GJ) is the heat price, *r* (%) is the discount rate with time ΔT(K) is the change in production temperature and η is the efficiency of the power plant. The values of *pp*, *pr* and *r* used in this research are reflecting prices in 2012 in Germany. It is worth mentioning that the pressure in both injection and production wells are updated as per each finite element simulation as well as during the optimisation process.

The third optimisation objective, which is the total cost (C_t) of the reservoir, can be calculated using Eq. 6:

$$C_t = C_w + C_e \quad (6)$$

In the present study, the long-term performance of EGS is achieved via maximising thermal power W_{hp} and minimising both the thermal drawdown *TD* and the total cost C_t using a bi-objective optimisation strategy. This was achieved using an EGS long-term performance criteria proposed by the Massachusetts Institute of Technology (MIT) report [38], which considers the reservoir not-productive when *TD* reaches 10%. In the optimisation algorithm proposed in this study, if the above condition is reached in the first ten years of heat extraction process, the design is considered to be redundant. In other words, objectives i and ii are combined and will form one objective of the optimisation process while the other objective will be the total cost.

2.2 Governing equations

In general, simulation of heat extraction in an EGS reservoir involves thermal-hydraulic-mechanical and chemical (THMC) coupled processes [39, 40]. However, the coupled hydraulic and thermal processes, which represent the fluid flow and heat transfer, play the most significant role in the heat extraction stage for the long-term performance compared to the other processes [41-43], see further discussion in Section 2.3.2.2. Thus, in this paper the mechanical and chemical processes have been ignored and only the fully coupled thermal-hydraulic (TH) processes are modelled to assess the long-term performance of EGS reservoir. Two energy equations are used to describe both the heat transfer in solid rock matrix (conductivity) and the heat transfer between the solid rock matrix and the fracture fluid (convection). The time-dependent heat transfer model requires the solution of two sets of differential equations representing the heat transfer in porous media (heat energy conservation) and the mass conservation (fluid flow equation).

2.2.1 Heat transfer:

Heat energy conservation and mass balance are the governing equations for the coupled TH processes involved in geothermal reservoir. The mathematical model of heat transfer in a porous medium is represented by Eqs. 7-10 [3]:

$$(\rho c_p)_{eff}\frac{\partial T}{\partial t} + \rho_w c_{p_f}\mathbf{u}.\nabla T + \nabla.\mathbf{q} = \mathrm{Q} \tag{7}$$

$$\mathbf{q} = -k_{eff}\nabla T \tag{8}$$

$$(\rho c_p)_{eff} = \theta\rho_w c_{p_f} + (1-\theta)\rho_r\, c_{p_r} \tag{9}$$

$$\mathrm{k}_{eff} = \theta k_f + (1-\theta)\mathrm{k}_r \tag{10}$$

Where ρ, ρ_f, ρ_r are the equivalent, fluid and rock matrix densities (kg/m^3) respectively; c_p, c_{p_f}, c_{p_r} are the equivalent, fluid and rock matrix heat capacities at constant pressure (J/(kg.^{o}C)) respectively; $(\rho c_p)_{eff}$ is the equivalent volumetric heat capacity at constant pressure; k_{eff}, k_f, k_r are the equivalent, fluid and rock matrix thermal conductivities (W/(m.^{0}C)) respectively; **u** is the Darcy velocity; T is the temperature (^{o}C); θ is the porosity of the rock matrix; Q is the heat source/sink term, and **q** is the conductivity heat flux of the rock matrix.

2.2.2 Fluid flow:

The mass conservation principle is applied to the hydraulic process. For mass balance, Darcy's Law is used assuming a laminar fluid flow. The mathematical model of fluid flow in a porous medium is represented by Eqs. 11-12 [3]:

$$\frac{\partial}{\partial t}(\theta\rho_f) + \nabla.(\rho_f\mathbf{u}) = Q_f \tag{11}$$

$$\mathbf{u} = -\frac{k}{\mu}\nabla p \tag{12}$$

where k is the permeability of the porous medium (m^2); μ the fluid dynamic viscosity (Pa.s); Q_f the fluid sink/source term, and p is the fluid pressure (Pa).

Equations (7) to (12) are solved using the finite element method. Details of the finite element model are presented in the next section.

2.3 The Finite Element Model (FEM)

The present research employs a single porosity model in which the geothermal reservoir is described as a porous medium with single porosity, taking into account both rock natural porosity and the presence of any fractures. In addition, the work presented in this paper considers an anisotropic equivalent permeability of the fractured zone.

2.3.1 Geometry and material properties

The Spa Urach geothermal reservoir in Germany is considered as a benchmark scenario for the present study due to the availability of the necessary data to re-create the finite element models [44]. A three-dimensional finite element model is developed to simulate the reservoir between 3,850 m and 4,150 m depth as shown in Figure 2. The temperature gradient is 0.03 ^{o}C/m and the reservoir is a doublet well system which consists of an injection and production wells at a separation distance of 400 m, see Figure 2. The equivalent fracture zone permeability is assumed to be 1.53e-15 (m^2) in the x direction and 3/8 of k_x in the y and z directions [45]. The material properties of the case study are presented in Table 1.

Figure 2. 3D geometry of the doublet well reservoir used in the FE model [45]

Table 1. Geometrical parameters and material properties of the FE model (adopted from [45]).

2.3.2 Initial and Boundary conditions

There are two sets of initial and boundary conditions in the present problem. The first set of initial and boundary values is related to the heat conduction process in the reservoir including the injection well. The second set of prescribed values consists of the initial and boundary conditions related to the hydraulic process in the reservoir, including prescribed pressures in the injection and production wells.

2.3.2.1 Initial conditions: The initial conditions related to both thermal and hydraulic processes are represented in Figure 3. The initial temperature in the reservoir is assumed to vary linearly with depth and a temperature gradient (T_g) of the Spa Urach site is 0.03 ^{o}C/m [45]. The reference temperature (T_{ref}) at a depth of 4445.0 m is 162 ^{o}C and the initial distribution of the temperature in the reservoir is given as a function of depth by Eq. 13 [45]:

$$T_o = T_{ref} + T_g(z - 4445) \tag{13}$$

Where, z is depth (m).

2.3.2.2 Boundary conditions: The fluid in the injection well is assumed to have a constant temperature of 50 ^{o}C as stated by McDermott *et al.* [46]. This corresponds to a Dirichlet boundary condition related to the heat conduction problem.

Fluid pressure in the injection well is assumed to have a prescribed value of 10 MPa at the top surface of the reservoir (over-pressurised fluid). This pressure increases linearly with depth as stated by McDermott *et al.* [46] according to Eq. 14. The production well is under-pressurised by -10 MPa on the top surface and linearly varies according to Eq. 15. On the lateral boundary of the reservoir, which is supposed to be at a large distance from the injection and production wells, both isothermal and hydrostatic conditions prevail during the whole time period. Hence, no fluid mass or heat flux take place through this boundary [47-49], which is enforced by the Neumann boundary conditions Eq. 16 and Eq. 17.

$$P_{inj} = \rho_f g z + 10 \text{ (MPa)} \tag{14}$$

$$P_{pro} = \rho_f g z - 10 \text{ (MPa)} \tag{15}$$

$$\mathbf{n} \cdot \rho_f \mathbf{u} = 0 \tag{16}$$

$$\mathbf{n} \cdot \mathbf{q} = 0 \tag{17}$$

Where, P_{inj} and P_{pro} are the injection and production fluid pressures (MPa) respectively, and **n** is the outward unit normal vector to the boundary.

Figure 3. Initial and boundary conditions for the numerical model [45]

2.3.3 Meshing

The FE mesh is refined around the wells to accommodate the high pressure and thermal gradients, as shown in in Figure 4. The mesh size grows outwards to the area surrounding the wells in order to achieve a reasonable computational time.

Figure 4. FE mesh of the proposed model and details of the mesh of the wells

Since the hybrid approach can involve millions of runs of FE models, particular attention is paid to the meshing to maintain the accuracy of the response while keeping a reasonable computational time. Four different mesh sizes were examined: mesh 1 is a coarse mesh which consists of 9709 elements, mesh 2 is finer than mesh 1, and has 16672 elements, mesh 3 is obtained after further refinement and has 23881 elements, and mesh 4 is a very fine mesh with 39920 elements. These cases were compared with respect to the production mass flow within 50 years of heat extraction, and the results are shown in Figure 5.

Figure 5. Mesh convergence with response to the production mass flow rate (graph corresponding to mesh 4 is covering curves 2 and 3)

From Figure 5, it is clear that once a certain mesh size is used, there is no further impact on the flow accuracy. As convergence is achieved with mesh 2, the mesh size corresponding to this mesh has been selected for the numerical simulations to be presented in the next sections (mesh 2, 3, and 4 are all providing relatively same curves at the scale presented in Figure 5 and as such it is not possible to distinguish between them).

2.4 Validation of the FE model

To demonstrate the accuracy of the FE modelling process, COMSOL Multiphysics [50] was used to replicate the numerical simulation of the Spa Urach geothermal reservoir as a validation problem. The results obtained with COMSOL Multiphysics (referred to as present work in Figure 6) are compared with those of [45] where GeoSys/RockFlow code [51] has been used in terms of a production temperature for a production period of 15 years. The three-dimensional transient FE analysis corresponding to this benchmark problem, is a fully THM coupled process. The fluid in the injection well has a pressure of 10MPa and a temperature of 50 °C and reservoir temperature gradient of 0.03 K/m is assumed. In general, the present results and those reported in [45] for the same problem are in close agreement, as can be seen in Figure 6. The small difference between the results can be attributed to the modelling of the injection and production wells which are discretised with one dimensional element 1D in Watanabe *et al.* [45] whereas, taking advantage of the problem symmetry, they could be modelled as two dimensional 2D half cylinder surfaces in the present study, see Figure 4.

Figure 6. Comparison of the present FE model and [45]

In addition to the above, the present FE model is also validated against the FE simulation conducted by Chen and Jiang [21] for an artificial reservoir to verify the TH coupled processes with a temperature gradient of 0.04 °C/m; an injection flow rate of 50 kg/s is considered at an injection temperature of 70 °C. The ground surface temperature is 27 °C. The reservoir has an equivalent permeability of 1e-14 m^2. The simulation of the TH coupled process is performed using a combination of the heat transfer in porous media and Darcy's Law modules in COMSOL Multiphysics. Hence, mechanical effects are neglected and the rock matrix is assumed to be rigid. Figure 7, indicates that the values of the production temperature from the FE model in this paper agree very closely with FE study conducted by [21] for 24 years of heat extraction.

Figure 7. Comparison of present FE modelling against [21]

3 Parametric study

A parametric study was performed to identify the key variables of the fitness function for the multi-objectives GA optimisation. The parametric study is limited to those variables of EGS reservoirs that are typically human-controlled (i.e. design parameters); which in this study, include reservoir depth, distance between injection and production wells, fluid injection pressure and temperature, and the equivalent permeability of both fracture and rock matrix network. Figure 8, shows the results of the parametric study. In these graphs, both objectives are normalised according to their maximum and minimum values; the breakthrough time varies from 0 to 50 years and the accumulative power varies from 0 to 200 MW, where these values were selected after a complete sensitivity analysis of the reservoir design parameters. As mentioned in Section 2 earlier, taking into consideration the threshold value of TD at 10 years of heat extraction, 0 for both normalised objectives will refer to the failure of the reservoir design before 10 years and 1 indicates the maximum values of the objectives.

The results are plotted for each key parameter while keeping other parameters constant at their reference values in Spa Urach project. The results show that the accumulative thermal power ($\sum W_{hp}$) is highly sensitive to the reservoir depth, well spacing, equivalent permeability of the fractured zone and the injection pressure. However, both objectives are less sensitive to the injection fluid temperature (Figure 8e). In addition, Figure 8a shows that the breakthrough time is less sensitive to the maximum reservoir depth. It is worth noting that, the maximum depth of the reservoir has significant impact on the drilling costs.

Figure 8. Sensitivity analysis for the EGS design parameters on both normalised thermal breakthrough time (dash line) and accumulative thermal power production (solid line) (all parameters are normalised with respect to their maximum values); where (a) reservoir depth, (b) distance between injection and production wells; (c) fluid injection pressure.; (d) equivalent permeability of the reservoir; (e) fluid injection temperature

Based on the sensitivity analysis, the maximum reservoir depth (D_h), distance between the injection and production wells (d), fractured zone permeability (k_x) and fluid injection pressure (P_{inj}) are selected to be the optimisation variables. The constraints for these variables are presented in Table 2.

Table 2. Constraints of the variables in GA multi-objectives

The following points were considered during selection of these constraints:

- The depth of the reservoir is estimated between 4000-6000 m. This range is assumed as it is more practical for drilling process [52].
- The distance between the injection and the production wells in rectangular reservoirs (which is the case in this research) depends on the industry considerations where the production and the injection wells should be at the centre of two adjacent circles, which have the same radius, equal to a half of the reservoir width [53], see Figure 9.

Figure 9. Industrial consideration for reservoir area based on the Influence zone of each well, after Wees *et al.* [53]

Therefore, based on the industrial consideration, the minimum boundaries of the injection and production wells are chosen to be at 150m distance from the reservoir edge.

- The permeability of the fractured zone has values within the range 10^{-13} m^2 – 10^{-16} m^2 [54].
- The injection pressure is varied between 1MPa to 20 MPa. The value of 20 MPa was determined after several initial trial and error simulations.

4 Results and discussions

An algorithm was developed to integrate FE analysis with a GA to find optimum values of the bi-objective fitness function. The first objective is to minimise the total reservoir cost and the second objective is to maximise the accumulative thermal power production ($\sum W_{hp}$) of the reservoir at the breakthrough time. As explained earlier in section 2.1, the thermal drawdown of the reservoir is implicitly considered in the latter by applying the threshold value of 10%TD during the optimisation process. The parameters of the Multi-objectives GA optimisation are summarised in Table 3. These values are chosen based on the number of variables, domain sizes and after a number of trial and errors simulations.

Table 3. Parameters used for the Multi-objective GA in the present research

Two scenarios are considered for the optimisation process. In the first scenario, all the design parameters (i.e. D_h, d, k and P_{inj}) are included during the optimisation of EGS design. The second scenario is carried out in order to determine the optimum solutions in the absence of any changes to the reservoir fracture configuration (i.e. without changing the equivalent permeability of the reservoir). For both scenarios, the GA-FE optimisation algorithm was run several times using different randomised initial points to ensure global optimum solutions are achieved. The following sections present the results of the two optimisation scenarios. The Pareto fronts of both scenarios are illustrated in Figure 10. Figures 10 (a, b) have been normalised to the minimum and maximum values of each scenario while Figure 10c is normalised with respect to the combined extreme values.

Figure 10. Pareto front of the optimum solutions of both scenarios (with and without changing the equivalent permeability of the reservoir), (a) 1st scenario, (b) 2nd scenario and (c) both case scenarios; where S11, S12 and S13 are the selected best designs in the 1st scenario and S21, S22 and S23 are the selected best designs in the 2nd scenario

Figure 10, show significant reduction in the value of the first objective (i.e. total cost) particularly in the first scenario. However, for the second objective (i.e. accumulative thermal power) there is no significant difference between the two scenarios, values of the second objective are restricted between

105-154 MW. In the first scenario, high accumulative thermal power designs have a cost between 75 to 88 Million $USA, as can be seen in Figure 10a. However, in the second scenario, to achieve a productive reservoir with high accumulative thermal power, a significantly higher investment is needed (about 110 to 185 Million $USA), see Figure 10b. Figure 10c presents the optimal trade-off curves of both case scenarios considered in the present study. The results show the considerable impact of permeability on the reservoir total cost. It is important to emphasize that this analysis has overlooked the cost of fracturing the reservoir and is only considering the two scenarios together to highlight the influence of permeability. The impact of the permeability on the other variables during the optimisation process, is presented in Figure 11, where the values of the optimised parameters are normalised to the selected constraints for the GA.

Figure 11. Maximum values of the normalised variables for both scenarios (with and without changing the equivalent permeability)

The results show that in the first scenario, when all the sensitive parameters vary within the given ranges, the reservoir extended to a moderate depth. This resulted into a lower drilling cost compared to the 2nd scenario, where the reservoir depth was much higher and corresponded to over 90% of the normalised depth. This depth was necessary to achieve a higher production temperature, which resulted into a higher drilling cost. In addition, both scenarios intend to reach about 0.9 of the normalised distance between the injection and production wells in order to sufficiently reduce the thermal breakthrough time. Furthermore, the maximum injection pressure in the second scenario is more than twice of that in the first scenario. The high injection pressure in the second scenario is due to the low permeability of the reservoir (about half of the maximum permeability of the first scenario) – this has a significant impact on increasing the operation cost.

The process of choosing the best solution from the Pareto front is something open for debate, to some extent subjective and most importantly depends on the design requirements for specific cases. In this paper, the minimum distance selection method (TMDSM), also known as Knee point, was used to find the best optimum solution that satisfies both objectives [55]. All the solutions on Pareto front in Figure 10 can be considered an optimum design for both scenarios, considering the circumstances and the design requirements. Should both objectives carry equal weights of importance, the minimum distance to a preferred point, which is (0, 0) in this study, is considered to select the best solution in the Pareto front. For the first and second scenarios these solutions are shown in Figures 10a and 10b (S11, S12, S13 and S21, S22, S23). For comparison, these solutions are presented in Figure 12. In this graph, normalised values of cost and power are both shown for all the cases and are compared with those of the benchmark case study of the Spa Urach geothermal reservoir. The optimum solutions are sorted with respect to the total costs.

Figure 12. Normalised power and cost of the selected best designs (S11, S12 and S13 from 1st scenario on Figure 10(a); S21, S22 and S23 from 2nd scenario on Figure 10(b) and the case study

In addition, the thermal evolution of two of the best solutions (S11 and S21) are compared to the case study in this research. It can be seen in Figure 13 that the cold water front in S11 and S21 did not reach the production well. However, the case study has reached the breakthrough time in early stages which means that the methodology presented in this paper is proven to be an efficient tool to obtain optimum designs for EGS reservoirs.

Figure 13. Thermal evolution of S11, S21 and the case study models

5 Conclusions

The purpose of the present study was to develop an advanced systematic approach to enhance long-term performance of EGS reservoirs. Given that the above is a complex problem that involves several factors, with inter-relationship between the factors and non-linear, nontrivial behaviour, it was not possible to use conventional approaches to achieve an optimum design. Therefore, in this research, an integration of FE analysis and GA optimisation technique was used to develop a methodology to find optimum designs of EGS reservoirs. This hybrid optimisation approach gives an insightful understanding of EGS long-term performance regarding the reservoir extraction efficiency, commercial feasibility and its service life. The research achieved the above objectives by combining both design and post-design models together.

From the results of the sensitivity analysis, it was shown that higher permeability of the fractured zone, higher fluid injection pressure and shorter distance between the injection and production wells can all produce higher thermal power at early stages. However, these parameters also have significant influences on the thermal drawdown and thus lead to the acceleration of the breakthrough time of EGS reservoirs. Therefore, there is a peak point for the accumulative thermal power when studying each of the above parameters. On the other hand, higher depth of EGS reservoir enhances the accumulative thermal power production, while it also results in high creation cost.

Taking into account the results of the sensitivity analysis, two scenarios (with and without changing the equivalent permeability of the reservoir) were considered during the optimisation process to find potential optimum design of EGS reservoirs. It was observed that the permeability of the reservoir has a significant influence on the required capital costs for EGS designs. The research also shows that there is a complex interaction between the reservoir design parameters, which might create challenges for decision makers regarding both design and post design stages. The proposed methodology, in this paper, can be used to transform the way EGS reservoirs are currently exploited leading to a sustainable use of these assets. Moreover, it has the flexibility and potential to be adapted during the operation of the EGS reservoir and/or as further information becomes available.

References

1. Grant, M., Geothermal reservoir engineering. 2013: Elsevier.

2. Olasolo, P., M. Juárez, M. Morales, and I. Liarte, Enhanced geothermal systems (EGS): A review. Renewable and Sustainable Energy Reviews, 2016. 56: p. 133-144.

3. Kolditz, O. and C. Clauser, Numerical simulation of flow and heat transfer in fractured crystalline rocks: application to the hot dry rock site in Rosemanowes (UK). Geothermics, 1998. 27(1): p. 1-23.

4. Duchane, D. and D. Brown, Hot dry rock geothermal energy development in the USA. Los Alamos National Laboratory, Los Alamos, NM, 2000.

5. BP, British Petroleum ,2015, online accessed 27th October 2016 http://www.bp.com/en/global/corporate/energy-economics/statistical-review-of-world-energy/renewable-energy/geothermal-power.html 2015.

6. Wang, G., K. Li, D. Wen, W. Lin, L. Lin, Z. Liu, W. Zhang, F. Ma, and W. Wang. Assessment of geothermal resources in China. in Proceedings, Thirty–Eighth Workshop on Geothermal Reservoir Engineering, Stanford University, Stanford, California, Febuary. 2013.

7. DECC, Deep Geothermal Review Study. 2013, Department of Energy and Climate Change.

8. GEA, Geothermal Energy Association (GEA). 2013, Geothermal.

9. Rybach, L. Legal and regulatory environment favourable for geothermal development investors. in Proceedings World Geothermal Congress 2010. 2010.

10. DiPippo, R., Geothermal power plants: principles, applications, case studies and environmental impact. 2012: Butterworth-Heinemann.

11. Giardini, D., Geothermal quake risks must be faced. Nature, 2009. 462(7275): p. 848-849.

12. Breede, K., K. Dzebisashvili, X. Liu, and G. Falcone, A systematic review of enhanced (or engineered) geothermal systems: past, present and future. Geothermal Energy, 2013. 1(1): p. 1-27.

13. Gringarten, A. and J. Sauty. The effect of reinjection on the temperature of a geothermal reservoir used for urban heating. in Proc. Second UN Symposium on the Development and Use of Geothermal Resources, San Francisco. 1975.

14. MacDonald, P., A. Stedman, and G. Symons. The UK geothermal hot dry rock R&D programme. in Seventeenth Workshop on Geothermal Reservoir Engineering. 1992.

15. Tenma, N., T. Yamaguchi, and G. Zyvoloski, The Hijiori hot dry rock test site, Japan: evaluation and optimization of heat extraction from a two-layered reservoir. Geothermics, 2008. 37(1): p. 19-52.

16. Mudunuru, M., S. Kelkar, S. Karra, D. Harp, G. Guthrie, and H. Viswanathan, Reduced-Order Models to Predict Thermal Output for Enhanced Geothermal Systems. 2016.

17. He, J., J. Sætrom, and L.J. Durlofsky, Enhanced linearized reduced-order models for subsurface flow simulation. Journal of Computational Physics, 2011. 230(23): p. 8313-8341.

18. Kruger, P. and B. Robinson. Heat extracted from the long term flow test in the Fenton Hill HDR reservoir. in NINETEENTH WORKSHOP GEOTHERMAL RESERVOIR ENGINEERING. 1994.

19. McClure, M.W. and R.N. Horne, An investigation of stimulation mechanisms in Enhanced Geothermal Systems. International Journal of Rock Mechanics and Mining Sciences, 2014. 72: p. 242-260.

20. Robinson, B.A. and J.W. Tester, Dispersed fluid flow in fractured reservoirs: An analysis of tracer-determined residence time distributions. Journal of Geophysical Research: Solid Earth, 1984. 89(B12): p. 10374-10384.

21. Chen, J. and F. Jiang, Designing multi-well layout for enhanced geothermal system to better exploit hot dry rock geothermal energy. Renewable Energy, 2015. 74: p. 37-48.

22. Bedre, M.G. and B.J. Anderson, Sensitivity analysis of low-temperature geothermal reservoirs: effect of reservoir parameters on the direct use of geothermal energy: Geothermal Resources Council Transactions. Geothermal Resources Council Transactions, 2012. 36: p. 1255-1261.

23. Chen, M., A.F. Tompson, R.J. Mellors, and O. Abdalla, An efficient optimization of well placement and control for a geothermal prospect under geological uncertainty. Applied Energy, 2015. 137: p. 352-363.

24. Biagi, J., R. Agarwal, and Z. Zhang, Simulation and optimization of enhanced geothermal systems using CO 2 as a working fluid. Energy, 2015. 86: p. 627-637.

25. Li, T., S. Shiozawa, and M.W. McClure, Thermal breakthrough calculations to optimize design of a multiple-stage Enhanced Geothermal System. Geothermics, 2016. 64: p. 455-465.

26. Aliyu, M.D. and H.-P. Chen, Sensitivity analysis of deep geothermal reservoir: Effect of reservoir parameters on production temperature. Energy, 2017. 129: p. 101-113.

27. Zhang, F.Z., Jiang, P.X. and Xu, R.N., 2013. System thermodynamic performance comparison of CO2-EGS and water-EGS systems. Applied Thermal Engineering, 61(2), pp.236-244.

28. Javadi, A.A., A. Faramarzi, and R. Farmani, Design and optimization of microstructure of auxetic materials. Engineering Computations, 2012. 29(3): p. 260-276.

29. Faramarzi, A., A.M. Alani, and O. Harireche, A hybrid approach to design materials with negative linear compressibility. Computational Materials Science, 2013. 79: p. 971-976.

30. Bödvarsson, G.S. and C.F. Tsang, Injection and thermal breakthrough in fractured geothermal reservoirs. Journal of Geophysical Research: Solid Earth, 1982. 87(B2): p. 1031-1048.

31. Pruess, K., Enhanced geothermal systems (EGS) using CO 2 as working fluid—a novel approach for generating renewable energy with simultaneous sequestration of carbon. Geothermics, 2006. 35(4): p. 351-367.

32. Tester, J., H. Herzog, Z. Chen, R. Potter, and M. Frank, Prospects for universal geothermal energy from heat mining. Science & Global Security, 1994. 5(1): p. 99-121.

33. Renner, J., The Future of Geothermal Energy. 2006, Idaho National Laboratory (INL).

34. Richards, H., R. Parker, A. Green, R. Jones, J. Nicholls, D. Nicol, M. Randall, S. Richards, R. Stewart, and J. Willis-Richards, The performance and characteristics of the experimental hot dry rock geothermal reservoir at Rosemanowes, Cornwall (1985–1988). Geothermics, 1994. 23(2): p. 73-109.

35. Tester, J.W. and H.J. Herzog, The economics of heat mining: An analysis of design options and performance requirements of hot dry rock (HDR) geothermal power systems. Energy Syst. Policy, 1991. 25: p. 33-63.

36. Lukawski, M.Z., B.J. Anderson, C. Augustine, L.E. Capuano, K.F. Beckers, B. Livesay, and J.W. Tester, Cost analysis of oil, gas, and geothermal well drilling. Journal of Petroleum Science and Engineering, 2014. 118: p. 1-14.

37. Kong, Y., Z. Pang, H. Shao, and O. Kolditz, Optimization of well-doublet placement in geothermal reservoirs using numerical simulation and economic analysis. Environmental Earth Sciences, 2017. 3(76): p. 1-7.

38. Tester, J.W., B. Anderson, A. Batchelor, D. Blackwell, R. DiPippo, E. Drake, J. Garnish, B. Livesay, M.C. Moore, and K. Nichols, The future of geothermal energy: Impact of enhanced geothermal systems (EGS) on the United States in the 21st century. Massachusetts Institute of Technology, 2006. 209.

39. Karrech, A., Non-equilibrium thermodynamics for fully coupled thermal hydraulic mechanical chemical processes. Journal of the Mechanics and Physics of Solids, 2013. 61(3): p. 819-837.

40. Taron, J. and D. Elsworth, Thermal–hydrologic–mechanical–chemical processes in the evolution of engineered geothermal reservoirs. International Journal of Rock Mechanics and Mining Sciences, 2009. 46(5): p. 855-864.

41. Bataillé, A., P. Genthon, M. Rabinowicz, and B. Fritz, Modeling the coupling between free and forced convection in a vertical permeable slot: Implications for the heat production of an Enhanced Geothermal System. Geothermics, 2006. 35(5): p. 654-682.

42. Finsterle, S., Y. Zhang, L. Pan, P. Dobson, and K. Oglesby, Microhole arrays for improved heat mining from enhanced geothermal systems. Geothermics, 2013. 47: p. 104-115.

43. Neuville, A., R. Toussaint, and J. Schmittbuhl, Fracture roughness and thermal exchange: A case study at Soultz-sous-Forêts. Comptes Rendus Geoscience, 2010. 342(7): p. 616-625.

44. Tenzer, H., U. Schanz, and G. Homeier. HDR research programme and results of drill hole Urach 3 to depth of 4440 m–the key for realisation of a hdr programme in southern Germany and northern Switzerland. in Proceedings World Geothermal Congress 2000. 2000.

45. Watanabe, N., W. Wang, C.I. McDermott, T. Taniguchi, and O. Kolditz, Uncertainty analysis of thermo-hydro-mechanical coupled processes in heterogeneous porous media. Computational Mechanics, 2010. 45(4): p. 263-280.

46. McDermott, C.I., A.R. Randriamanjatosoa, H. Tenzer, and O. Kolditz, Simulation of heat extraction from crystalline rocks: The influence of coupled processes on differential reservoir cooling. Geothermics, 2006. 35(3): p. 321-344.

47. Pashkevich, R.I. and V.V. Taskin. Numerical simulation of exploitation of supercritical enhanced geothermal system. in Proceedings of thirty-fourth workshop on geothermal reservoir engineering. Stanford (California): Stanford University. 2009.

48. Sanyal, S.K. and S.J. Butler, An analysis of power generation prospects from enhanced geothermal systems. Geothermal Resources Council Transactions, 2005. 29.

49. Vörös, R., R. Weidler, L. de Graaf, and D. Wyborn. THERMAL MODELLING OF LONG TERM CIRCULATION OF MULTI-WELL DEVELOPMENT AT THE COOPER BASIN HOT FRACTURED ROCK (HFR) PROJECT AND CURRENT PROPOSED SCALE-UP PROGRAM. in Proceedings of the Thirty-Second Workshop on Geothermal Reservoir Engineering, Stanford, CA, USA. 2007.

50. COMSOL-Multiphysics, INTRODUCTION TO COMSOL Multiphysics: Version 5.2a. Stockholm, Sweden: COMSOL AB. 2016.

51. Kolditz, O. and H. Shao, Developer Benchmark Book on THMC Components of Numerical Codes GeoSys/Rockflow V. 4.9. Helmholtz Centre for Environmental Research (UFZ), Leipzig, 2009.

52. Heidinger, P., Integral modeling and financial impact of the geothermal situation and power plant at Soultz-sous-Forêts. Comptes Rendus Geoscience, 2010. 342(7): p. 626-635.

53. van Wees, J., L. Kramers, R. Kronimus, M. Pluymaekers, H. MijnLieff, and G. Vis, ThermoGIS TM V1. 0 Part II: Methodology. 2010.

54. Kosack, C., C. Vogt, V. Rath, and G. Marquart. Stochastic estimates of the permeability field of the Soultz-sous-Forêts geothermal reservoir-comparison of Bayesian inversion, MC geostatistics, and EnKF assimilation. in EGU General Assembly Conference Abstracts. 2010.

55. Hussain, M.S., Numerical Simulation and Effective Management of Saltwater Intrusion in Coastal Aquifers, PhD Thesis, University of Exeter, 2015.

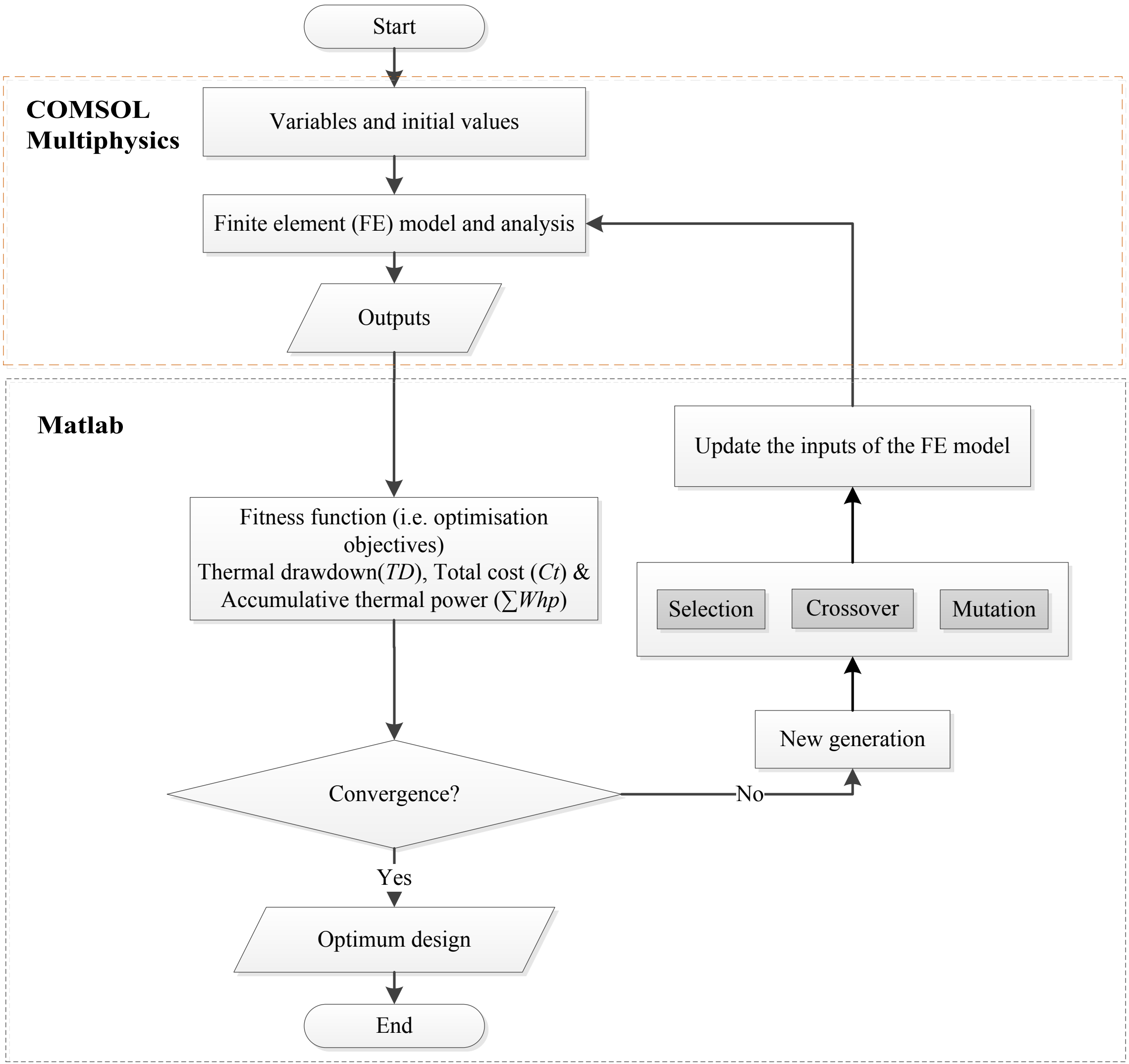

Figure 1. Flowchart for the integration of FE Analysis with Multi-objective GA

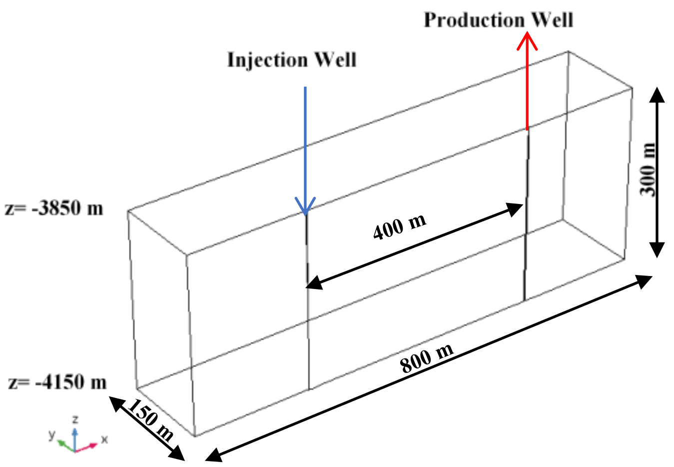

Figure 2. 3D geometry of the doublet well reservoir used in the FE model [44]

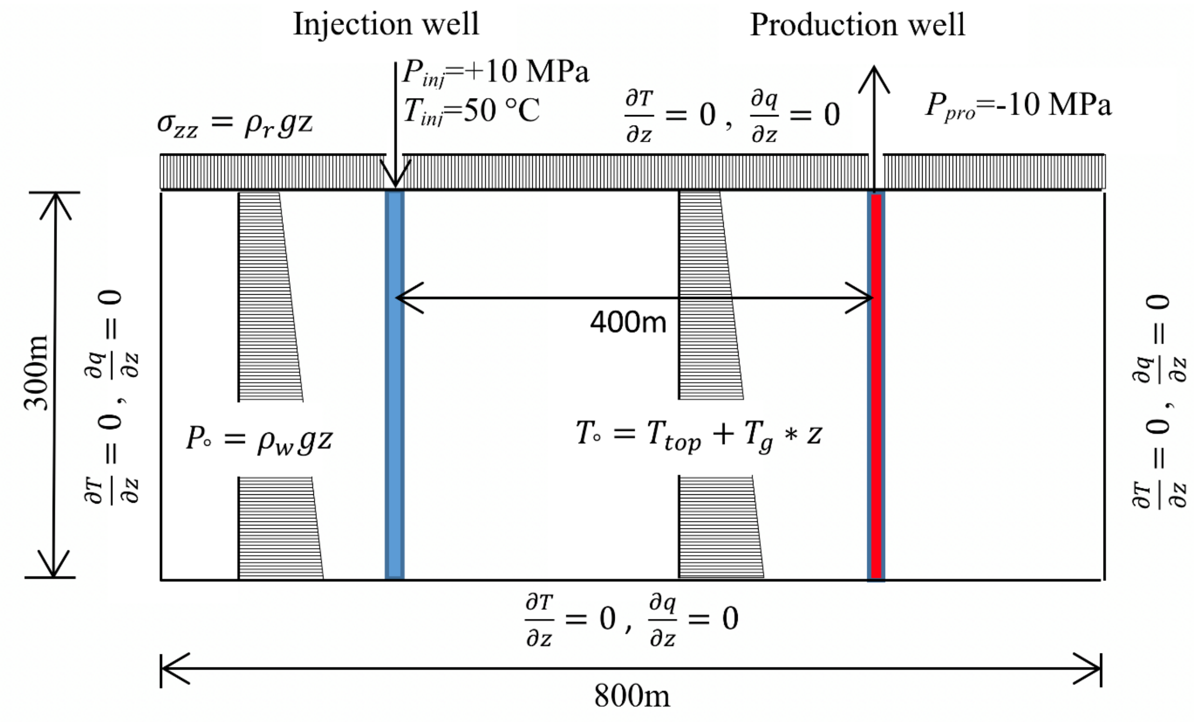

Figure 3. Initial and boundary conditions for the numerical model [44]

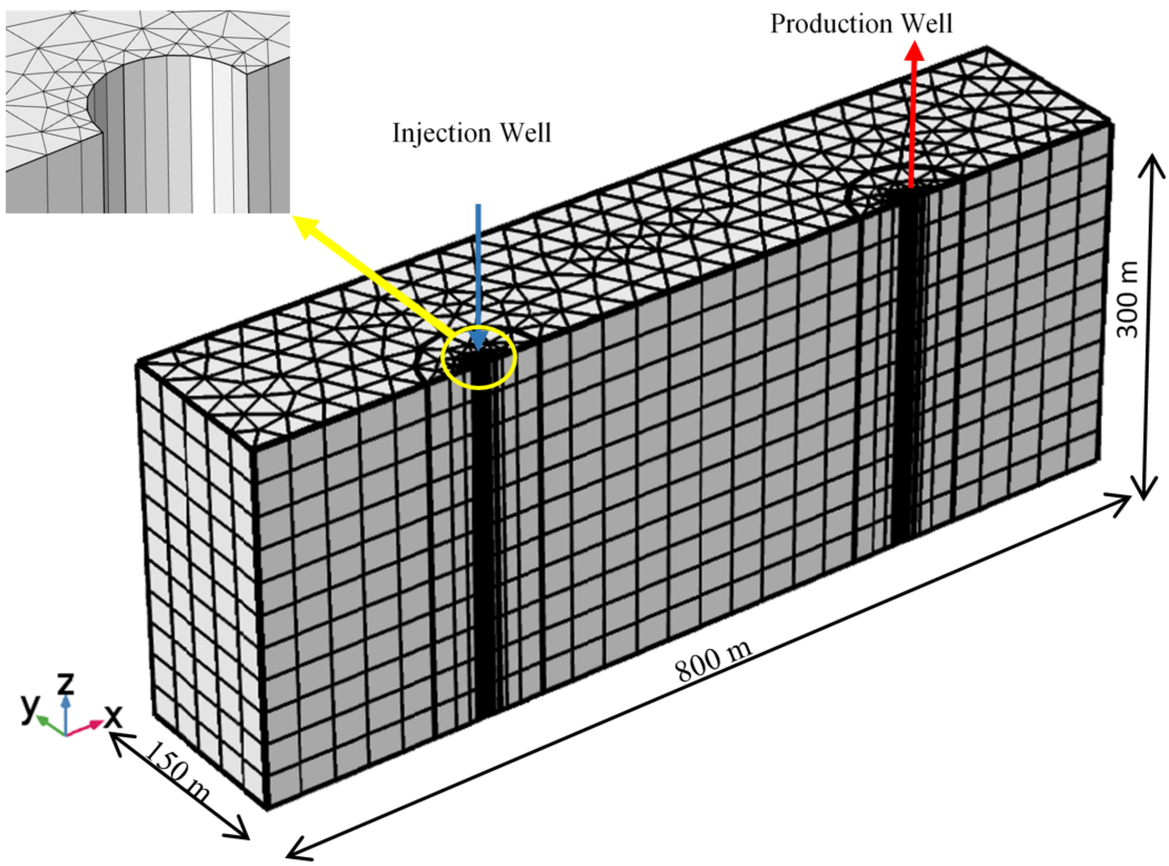

Figure 4. FE mesh of the proposed model and details of the mesh of the wells

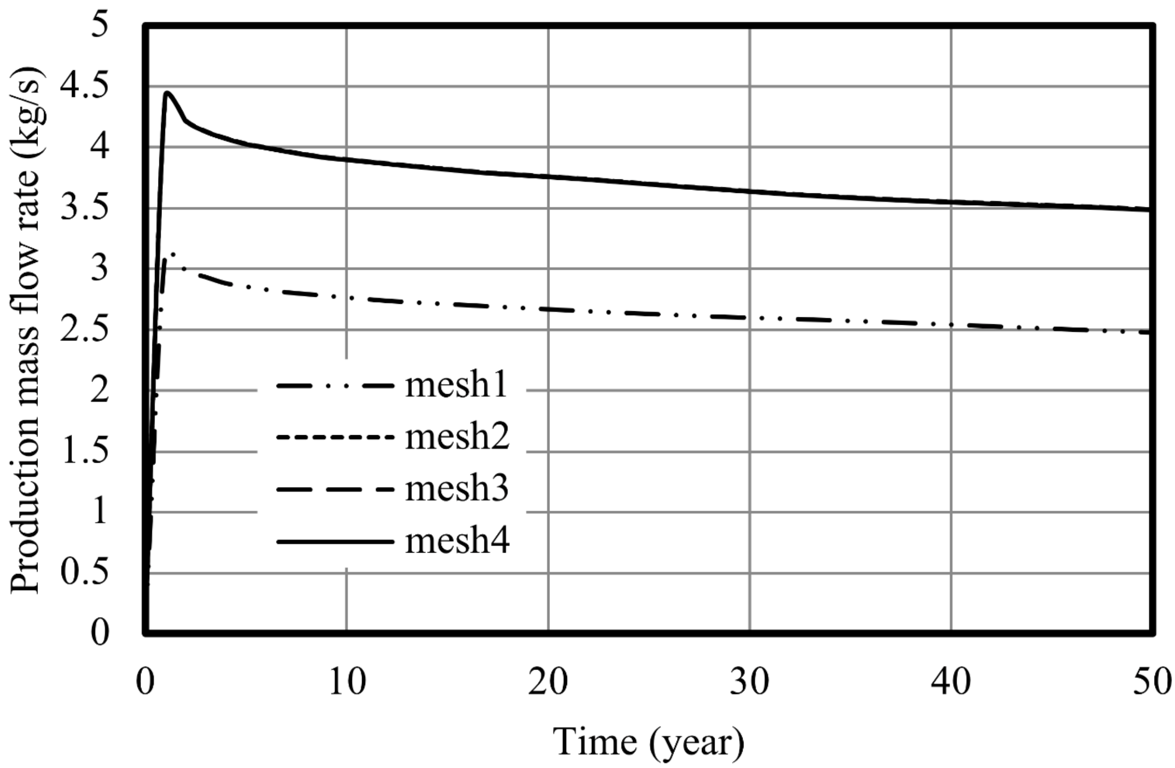

Figure 5. Mesh convergence with response to the production mass flow rate (graph corresponding to mesh 4 is covering curves 2 and 3)

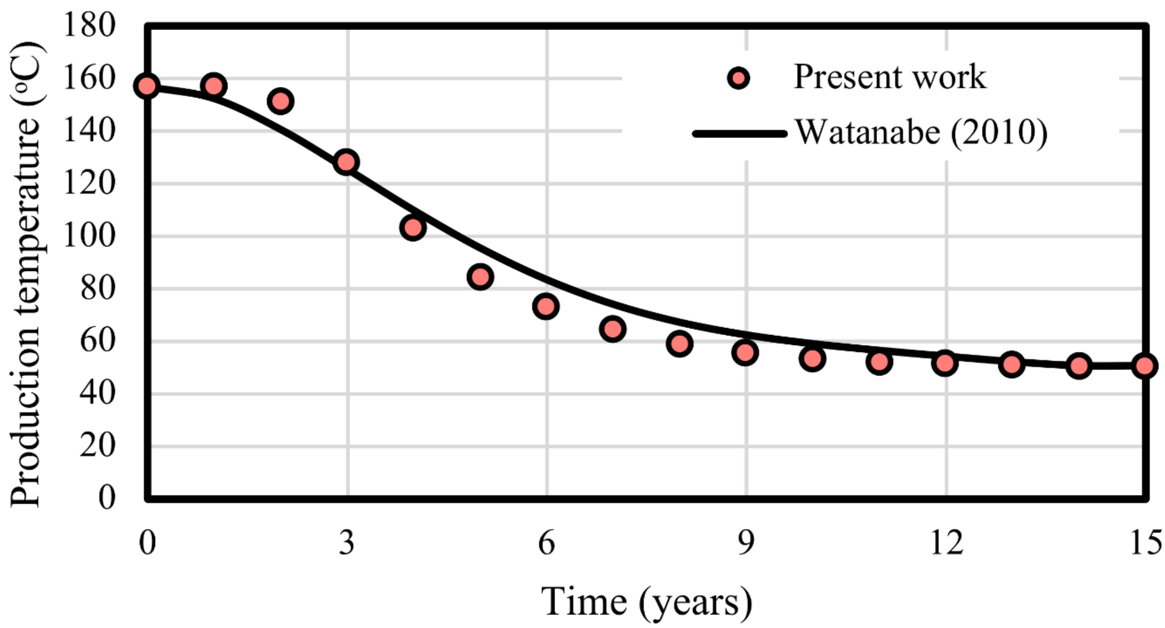

Figure 6. Comparison of the present FE model and [44]

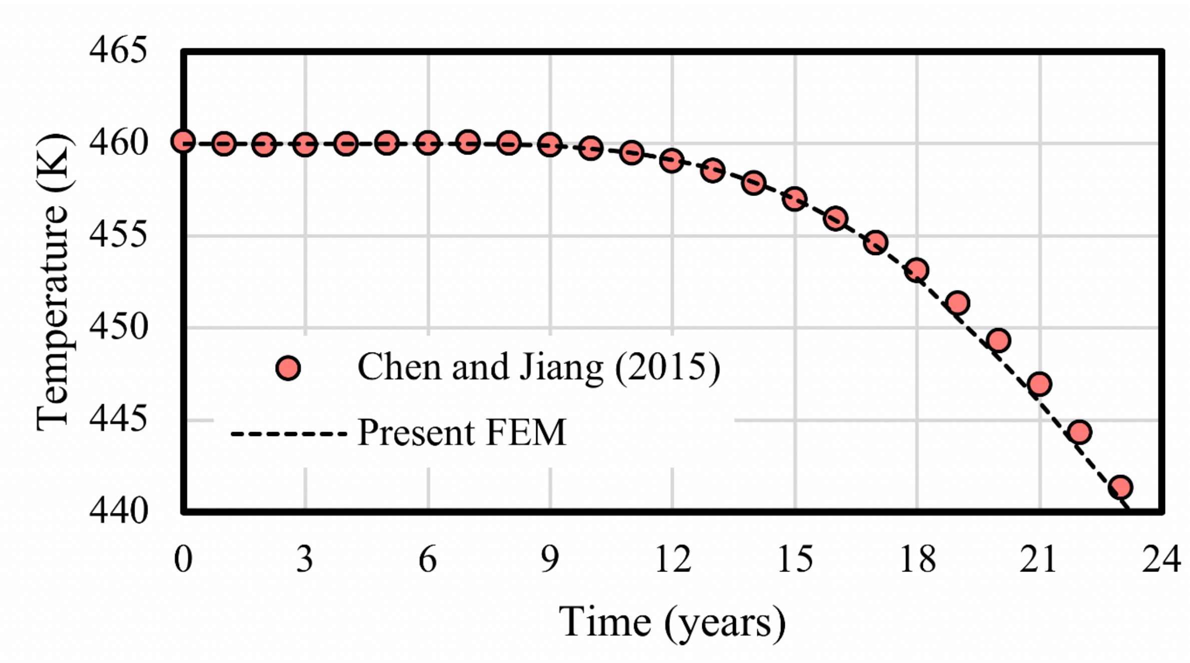

Figure 7. Comparison of present FE modelling against [21]

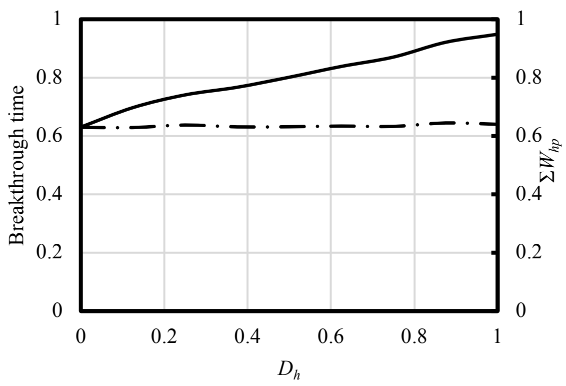

(a)

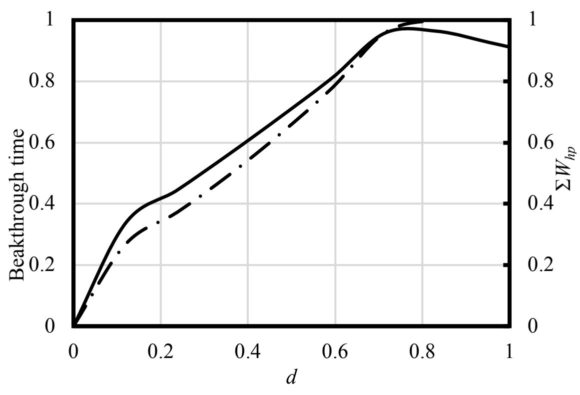

(b)

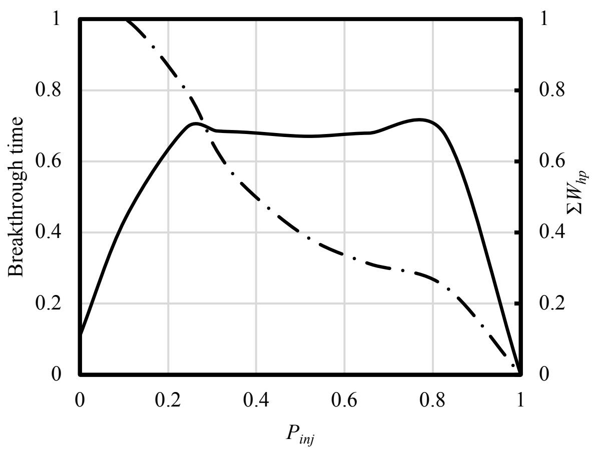

(c)

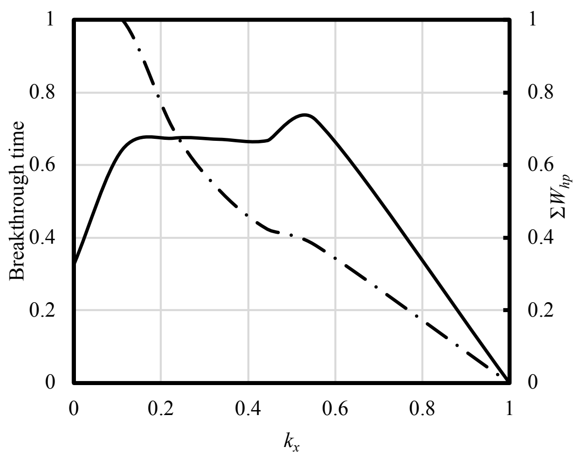

(d)

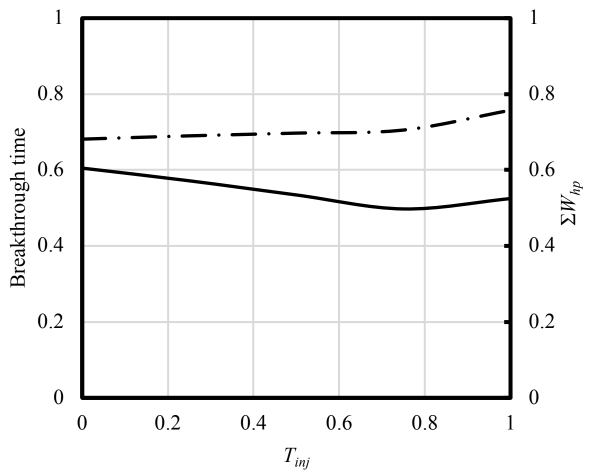

(e)

Figure 8. Sensitivity analysis for the EGS design parameters on both normalised thermal breakthrough time (dash line) and accumulative thermal power production (solid line) (all parameters are normalised with respect to their maximum values); where (a) reservoir depth, (b) distance between injection and production wells; (c) fluid injection pressure.; (d) equivalent permeability of the reservoir; (e) fluid injection temperature

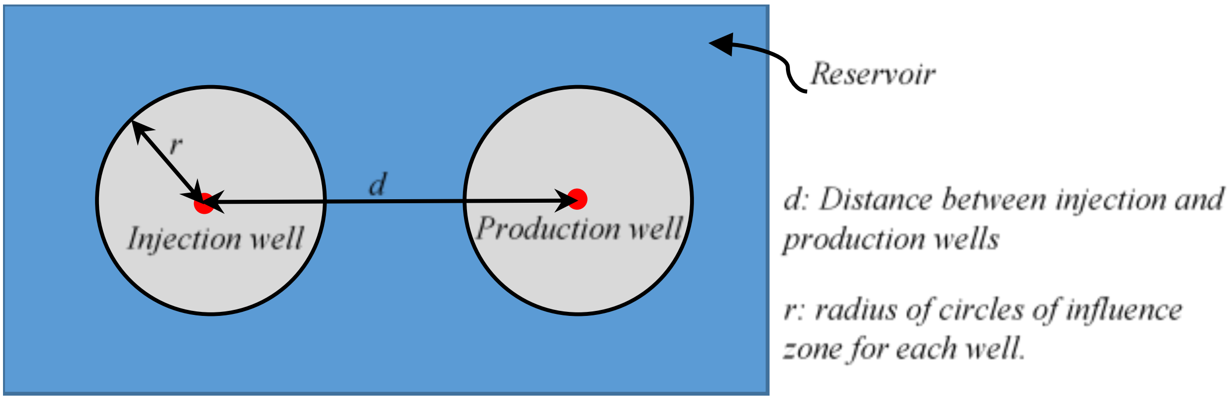

Figure 9. Industrial consideration for reservoir area based on the Influence zone of each well, after Wees *et al.* [52]

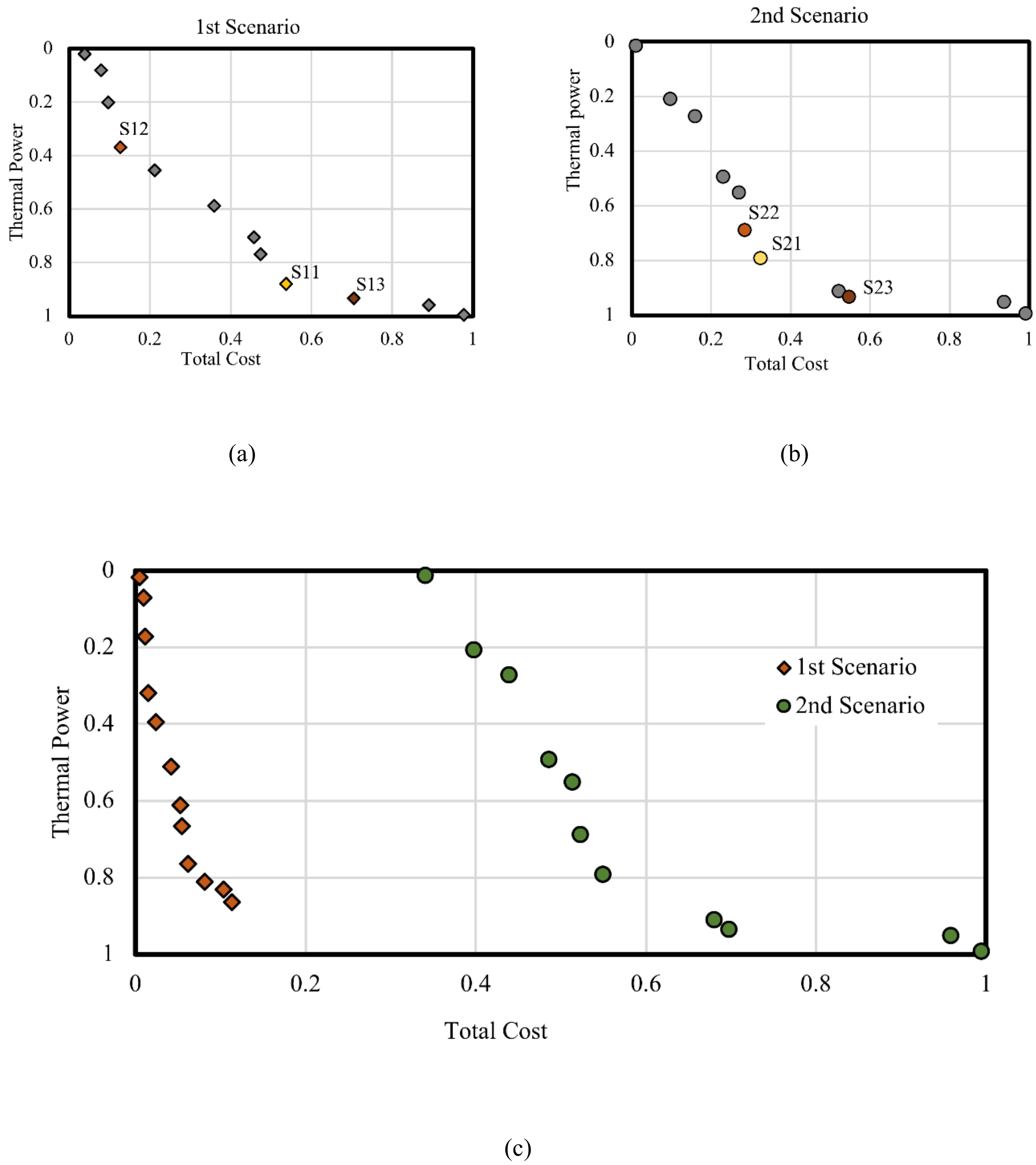

Figure 10. Pareto front of the optimum solutions of both scenarios (with and without changing the equivalent permeability of the reservoir), (a) 1st scenario, (b) 2nd scenario and (c) both case scenarios; where S11, S12 and S13 are the selected best designs in the 1st scenario and S21, S22 and S23 are the selected best designs in the 2nd scenario

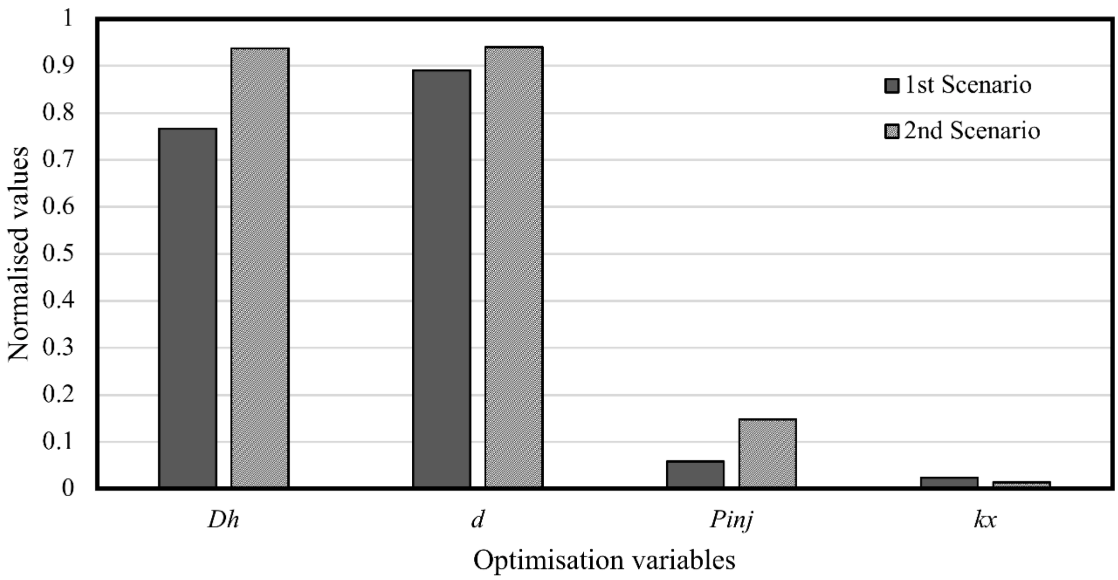

Figure 11. Maximum values of the normalised variables for both scenarios (with and without changing the equivalent permeability)

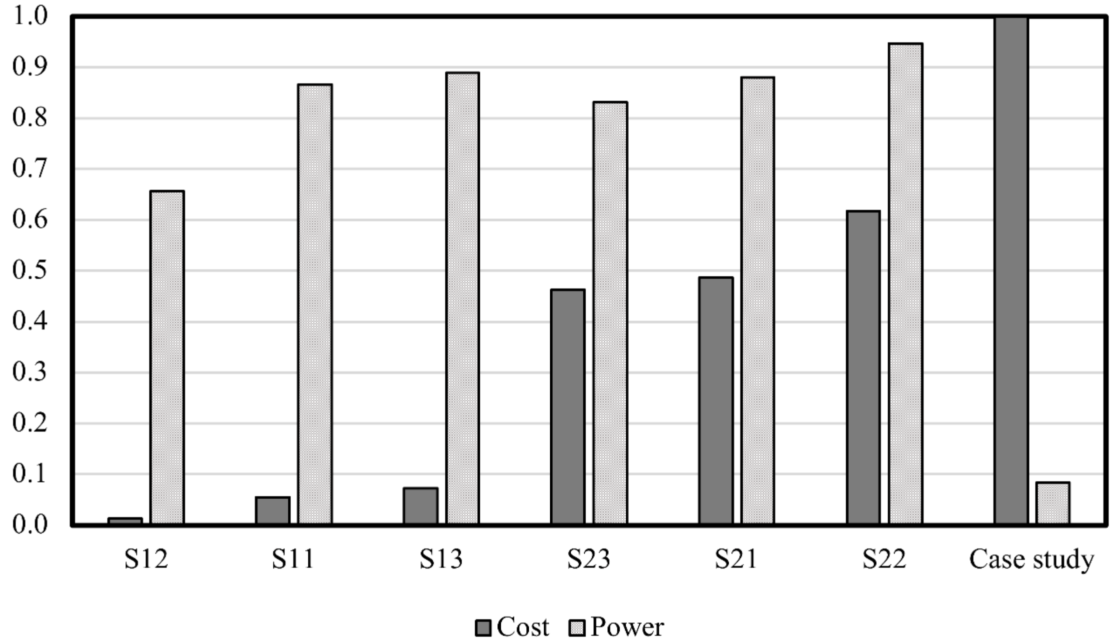

Figure 12. Normalised power and cost of the selected best designs (S11, S12 and S13 from 1st scenario on Figure 10(a); S21, S22 and S23 from 2nd scenario on Figure 10(b) and the case study

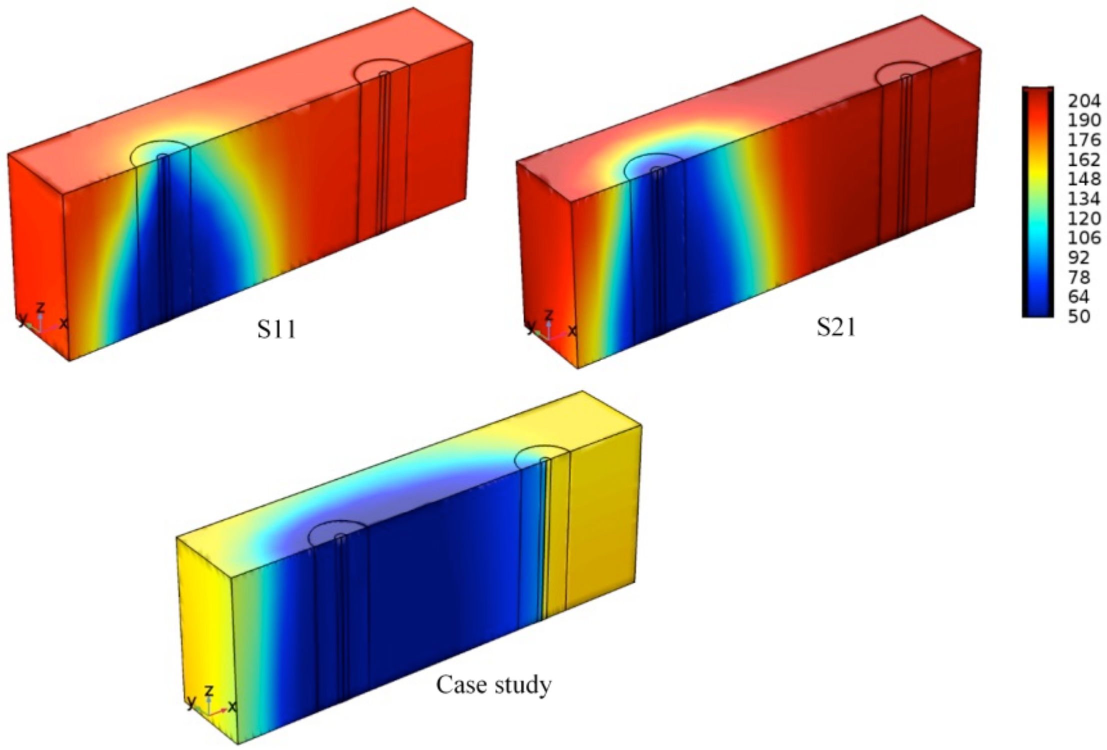

Figure 13. Thermal evolution of S11, S21 and the case study models

Table 1. Geometrical parameters and material properties of the FE model (adopted from [44]).

	Parameters	*Symbols*	Value	Unit
Rock matrix	Domain length	L_r	800	m
	Domain width	W_r	300	m
	Domain height	H_r	300	m
	Reservoir surface depth	D_s	3850	m
	Reservoir base depth	D_h	4150	m
	Density	ρ_r	2750	kg/m^3
	Permeability	k	k_x=1.53e-15, k_y=k_z=3/8*k_x	m^2
	Porosity	$\emptyset$	0.005	
	Specific heat capacity	c_{p_r}	850	J/(kg.^{o}C)
	Thermal conductivity	k_r	3	W/(m.^{0}C)
Injection fluid	Density	ρ_f	1000	kg/m^3
	Specific heat capacity	c_{p_f}	4210	J/(kg.^{o}C)
	Thermal conductivity	k_f	0.6	W/(m.^{o}C)
	Dynamic viscosity	μ	2e-4	Pa.s
Others	Well length	L_w	300	m
	Well diameter	d_w	1	m
	Well separation distance	d	400	m
	Reference temperature at 4445.0 m	T_{ref}	162	^{o}C
	Temperature gradient	T_g	0.03	^{o}C/m

Table 2. Constraints of the variables in GA multi-objectives

Constraints	Variables			
	Maximum reservoir depth (D_h)[a]	Well positions (d)[b]	Fracture zone permeability (k_x)[c]	Injection fluid pressure (P_{inj})[d]
	m	m	m^2	MPa
Lower bound	4000	300	1e-13	1
Upper bound	6000	500	1e-16	20

Note: values cited are based on a) [51], b) [52], c) [53] and d) trial and errors.

Table 3. Parameters used for the Multi-objective GA in the present research

Number of Populations	50
Maximum generation number	400
Selection	Tournament size 2
Crossover	0.7
Mutation	Constraint dependent